

Millennial meridional dynamics of IPWP during the last termination

L. Lo et al.

Title Page

Abstract

Introduction

Conclusions

References

Tables

Figures



Back

Close

Full Screen / Esc

Printer-friendly Version

Interactive Discussion



(G/IG) cycles, and to constrain the relationship between warm pool thermal and hydrological fluctuations to high latitude ice sheet and greenhouse gas concentrations during the late Pleistocene (e.g., Lea et al., 2000; Stott et al., 2002; Visser et al., 2003; Rosenthal et al., 2003; Stott et al., 2004; de Garidel-Thoron et al., 2005; Steinke et al., 2006; Levi et al., 2007; Xu et al., 2008; Linsley et al., 2010; Bolliet et al., 2011; Mothadi et al., 2014).

Stacked IPWP SST and seawater oxygen isotope ($\delta^{18}\text{O}_{\text{SW}}$) records from the last glacial to the Holocene clearly show a close link between the IPWP SST, the Asian-Australian Monsoon (AAM) system, and sea level (Stott et al., 2004; Oppo et al., 2009; Linsley et al., 2010). However, a complicated ocean–island configuration and regional topography hinder the fidelity of using these records to describe past climate changes in detail (Griffiths et al., 2009; Mohtadi et al., 2011). In particular, little is known about the meridional thermal-hydrological dynamics between the N- and S-IPWP during the last termination.

Here we present new oceanic proxy-inferred SST and ice volume-corrected surface seawater oxygen isotope $\delta^{18}\text{O}$ ($\delta^{18}\text{O}_{\text{SW-IVC}}$) records from the Solomon Sea, Papua New Guinea (PNG) for the past 23–10.5 thousand years ago (ka, before 1950 AD, hereafter). New SST and $\delta^{18}\text{O}_{\text{SW-IVC}}$ stacked records since the last termination are built for both the N- and S-IPWP to understand regional thermal-hydrological changes and interhemispheric teleconnections.

2 Material and methods

Site MD05-2925 (9.3° S, 151.5° E, water depth 1661 m) is located at the northern slope of the Woodlark Basin in the Solomon Sea, which is the passage of surface and sub-surface water masses between low- and middle-latitude South Pacific Ocean gyre and cross equatorial currents (Grenier et al., 2011; Melet et al., 2011) (Fig. 1). The seasonal precipitation in this region (Fig. 1) is dominated by the AAM system, coupled with the intertropical convergence zone (ITCZ) (Shiau et al., 2012, and references therein).

Millennial meridional dynamics of IPWP during the last termination

L. Lo et al.

Title Page

Abstract

Introduction

Conclusions

References

Tables

Figures



Back

Close

Full Screen / Esc

Printer-friendly Version

Interactive Discussion



The empirical orthogonal function (EOF) analysis of a modern SST dataset (1950–2004 AD, Reynolds et al., 2002) for a sector from 20° S–20° N, and 100–180° E was conducted (Fig. 2) to determine the boundary between N- and S-IPWP. With an equatorial border, the EOF1 factor (83.4 %) clearly resolved different SST variation groups. The EOF2 factor shows minor (9.7 %) but significant inter-annual zonal (ENSO) control on the SST patterns. EOF results show that the geographic equator is also the thermal equator between N-IPWP and S-IPWP (Fig. 2).

To build a stacked N- and S-IPWP record, we followed the suggestions by Leduc et al. (2010) and considered two criteria for this dataset: (1) sites with locations from 12° N to 15° S, which is the main IPWP range (Yan et al., 1992; Gagan et al., 2004), and (2) usage of specific proxies, Mg / Ca-derived SST and $\delta^{18}\text{O}_\text{C}$ records of planktonic foraminifera, *G. ruber* (white, s.s.). Records from 12 sites were selected, including this study (Table 2). We adopted an age model for sites ODP806, MD97-2140, MD97-2141, MD98-2162, MD98-2170, MD98-2176, and MD98-2181. For records with available original radiocarbon ages from sites, including MD01-2378, MD01-2390, MD98-2165, and MD06-3067, we recalculated the age models using the CALIB 6.0.1 program. The sea level change effect on $\delta^{18}\text{O}_\text{SW}$ was also corrected. We divided the total data into 400 yr windows and calculated the mean and standard error of the mean for each time window.

3 Results and discussion

3.1 Geochemical proxy data at site MD05-2925

Planktonic foraminiferal geochemical proxy data for site MD05-2925 are shown in Fig. 3. *G. ruber* $\delta^{18}\text{O}_\text{C}$ varies from -1.0 to -2.3 ‰ and shows no significant millennial timescale variations. Mg / Ca ratios feature stable glacial values of ~ 3.5 mmol mol⁻¹ and rapid increasing transitions of 0.5–1.0 mmol mol⁻¹ at ~ 18.5 , 16.5, 14.5, and

Millennial meridional dynamics of IPWP during the last termination

L. Lo et al.

[Title Page](#)[Abstract](#)[Introduction](#)[Conclusions](#)[References](#)[Tables](#)[Figures](#)[Back](#)[Close](#)[Full Screen / Esc](#)[Printer-friendly Version](#)[Interactive Discussion](#)

The thermal gradient between N- and S-IPWP is around 1 °C during 23 to 19 ka. Due to the earlier S-IPWP warming, the thermal gradient dropped from 1 to 0.5 °C around 19–18 ka, and persisted to the end of the H1 event. The largest observed thermal gradient (1.5–2.0 °C) occurred during the B/A period, and was followed by a 1 °C drop during the YD. The meridional SST gradient between N- and S-IPWP over the last termination is attributed to the large thermal variability in the S-IPWP (Fig. 5a). Asynchronicity between persistent N-IPWP and fluctuating S-IPWP SST sequences (Fig. 5a) indicates a meridionally dynamic IPWP through the last termination period. This N–S SST gradient variability would also affect interhemispheric air flow and heat transport (Gibbons et al., 2014; McGee et al., 2014), providing a mechanism to explain heat transport between the hemispheres on a millennial timescale.

3.4 N- and S-IPWP $\delta^{18}\text{O}_{\text{SW-IVC}}$ records

Both N- and S-IPWP $\delta^{18}\text{O}_{\text{SW-IVC}}$ records feature (i) high values of 0.8–1.2‰ during glacial times, and (ii) a decreasing trend after 17–16 ka (Fig. 5c). The gradient between N- and S-IPWP gradually increased from 0‰ to 0.2‰ through the termination (Fig. 5d). A similar pattern of $\delta^{18}\text{O}_{\text{SW-IVC}}$ between N- and S-IPWP suggests that hydrological conditions in the two regions were governed by the same factor(s), probably related to Northern Atlantic cold perturbations (Shakun and Carlson, 2010). It has also been suggested that a major $\delta^{18}\text{O}_{\text{SW-IVC}}$ increase in the IPWP region likely resulted from reduced precipitation and oceanic advection in both the N-IPWP and S-IPWP regions (Gibbons et al., 2014; McGee et al., 2014).

3.5 Meridional IPWP SST gradient and the southward-shifted ITCZ precipitation boundary

A striking feature of the stacked SST records is the warming in the S-IPWP during the H1 and YD periods (Fig. 5a). Modern observatory data over the past six decades (Fig. 12 of Feng et al., 2013) show that an equatorward shift of the NH convection

To sum up our geochemical and composite dataset in the IPWP region during the last terminations, we propose that the enlarged IPWP meridional SST gradient could result in an altered HC and reduced (increased) precipitation for the East Asian (Australia) monsoon territories during the H1 and YD periods (McGee et al., 2014). We also propose that variations in the meridional IPWP SST gradient during the termination period were mainly caused by the S-IPWP, which is closely linked to high-latitude climate systems.

4 Conclusions

Our new MD05-2925 marine geochemical records and previous reports suggest that the meridional IPWP thermal conditions are strongly linked to interhemispheric high-latitude climate during the last deglaciation. Ice volume-corrected $\delta^{18}\text{O}_{\text{SW}}$ stacked records show an increasing salinity gradient between N- and S-IPWP over the last termination. Here we propose a new process of the thermal evolution of IPWP region, which meridional differences of its thermal gradient could amplify the signal from both hemispheric climate event and greenhouse gas concentration. A hypothetical precipitation boundary around 8–10° S during H1 and the YD has also been proposed, which is most likely caused by the meridional IPWP SST gradient and HC circulation anomalies. More advanced high-resolution regional model simulations are required to clarify the role of IPWP meridional thermal-hydrological gradient to an altered HC and its relationship with regional and global climate systems during global climate perturbation events.

CPD

10, 3397–3419, 2014

Millennial meridional dynamics of IPWP during the last termination

L. Lo et al.

Title Page

Abstract

Introduction

Conclusions

References

Tables

Figures

◀

▶

◀

▶

Back

Close

Full Screen / Esc

Printer-friendly Version

Interactive Discussion



Acknowledgements. MD05-2925 site location was selected by Min-Te Chen and Meng-Yang Lee and collected during the IMAGES PECTEN Cruise, conducted by Luc Beaufort and Min-Te Chen. Chien-Ju Chou, Wan-Lin Hu, and Yu-Ting Hsiao helped to pick foraminifera samples. Yang-Hui Hsu helped to operate the climatological database and plotted figures. Thanks to Delia W. Oppo and Braddock K. Linsley for their generous offering of the non-overlapping method MatLab code. This research was funded by Taiwan ROC MOST (98-2811-M-002-129, 99-2611-M-002-005, 100-2116-M-002-009 to CCS, and 95-2611-M-002-019, 96-2611-M-002-019 to KYW), and National Taiwan University (101R7625 to CCS).

References

- Ayliffe, L. K., Gagan, M. K., Zhao, J.-X., Drysdale, R. N., Hellstrom, J. C., Hantoro, W. S., Griffiths, M. L., Scott-Gagan, H., Pierre, E. S., Cowley, J. A., and Suwargadi, B. W.: Rapid interhemispheric climate links via the Australasian monsoon during the last deglaciation, *Nat. Commun.*, 4, 2908, doi:10.1038/ncomms3908, 2013.
- Bolliet, T., Holbourn, A., Kuhnt, W., Laj, C., Kissel, C., Beaufort, L., Kienast, M., Andersen, N., and Garbe-Schönberg, D.: Mindanao Dome variability over the last 160 kyr: episodic glacial cooling of the West Pacific Warm Pool, *Paleoceanography*, 26, PA1208, doi:10.1029/2010PA001966, 2011.
- Broccoli, A. J., Dahl, K. A., and Stouffer, R. J.: Response of the ITCZ to Northern Hemisphere cooling, *Geophys. Res. Lett.*, 33, L01702, doi:10.1029/2005GL024546, 2006.
- Carolin, S. A., Cobb, K. M., Adkins, J. F., Clark, B., Conroy, J. L., Lejau, S., Malang, J., and Tuen, A. A.: Varied response of Western Pacific hydrology to climate forcings over the last glacial period, *Science*, 340, 1564–1566, 2013.
- Chiang, J. C. H. and Bitz, C. M.: Influence of high latitude ice cover on the marine Intertropical Convergence Zone, *Clim. Dynam.*, 25, 477–496, 2005.
- Cravatte, S., Delcroix, T., Zhang, D., McPhaden, M., and Leloup, J.: Observed freshening and warming of the western Pacific Warm Pool, *Clim. Dynam.*, 33, 565–589, 2009.
- de Garidel-Thoron, T., Rosenthal, Y., Bassinot, F., and Beaufort, L.: Stable sea surface temperatures in the western Pacific warm pool over the past 1.75 million years, *Nature*, 433, 294–298, 2005.

Millennial meridional dynamics of IPWP during the last termination

L. Lo et al.

[Title Page](#)

[Abstract](#)

[Introduction](#)

[Conclusions](#)

[References](#)

[Tables](#)

[Figures](#)

[⏪](#)

[⏩](#)

[◀](#)

[▶](#)

[Back](#)

[Close](#)

[Full Screen / Esc](#)

[Printer-friendly Version](#)

[Interactive Discussion](#)



- Feng, J., Li, J., and Xie, F.: Long-term variation of the principal mode of boreal spring Hadley Circulation linked to SST over the Indo-Pacific Warm Pool, *J. Climate*, 26, 532–544, 2013.
- Gibbons, F. T., Oppo, D. W., Mohtadi, M., Rosenthal, Y., Cheng, J., Liu, Z., and Linsley, B. K.: Deglacial $\delta^{18}\text{O}$ and hydrological variability in the tropical and Indian Oceans, *Earth Planet. Sc. Lett.*, 387, 240–251, 2014.
- Grenier, M., Cravatte, S., Blanke, B., Menkes, C., Joch-Larrouy, A., Durand, F., Melet, A., and Jeandel, C.: From the western boundary currents to the Pacific Equatorial Undercurrent: modeled pathways and water mass evolutions, *J. Geophys. Res.*, 116, C12044, doi:10.1029/2011JC007477, 2011.
- Griffiths, M. L., Drysdale, R. N., Gagan, M. K., Zhao, J.-X., Ayliffe, L. K., Hellstrom, J. C., Hantoro, W. S., Frisia, S., Feng, Y.-X., Cartwright, I., St. Pierre, E., Fischer, M., J., and Suwargadi, B. W.: Increasing Australian–Indonesian monsoon rainfall linked to early Holocene sea-level rise, *Nat. Geosci.*, 2, 636–639, 2009.
- Lamy, F., Kaiser, J., Ninnemann, U., Hebbeln, D., Arz, H. W., and Stoner, J.: Antarctic timing of surface water changes off Chile and Patagonian ice sheet response, *Science*, 304, 1959–1962, 2004.
- Lea, D. W., Pak, D. K., and Spero, H. J.: Climate impact of late Quaternary equatorial Pacific sea surface temperature variations, *Science*, 289, 1719–1724, 2000.
- Lea, D. W., Pak, D. K., Peterson, L. C., and Hughen, K. A.: Synchronicity of tropical high-latitude Atlantic temperatures over the last glacial termination, *Science*, 301, 1361–1364, 2003.
- Leduc, G., Schneider, R., Kim, J. H., and Lohmann, G.: Holocene and Eemian sea surface temperature trends as revealed by alkenone and Mg/Ca paleothermometry, *Quaternary Sci. Rev.*, 29, 989–1004, 2010.
- Levi, C., Labeyrie, L., Bassinot, F., Guichard, F., Cortijo, E., Waelbroeck, C., Caillon, N., Duprat, J., de Garidel-Thoron, T., and Elderfield, H.: Low-latitude hydrological cycle and rapid climate changes during the last deglaciation, *Geochem. Geophys. Geosy.*, 8, Q05N12, doi:10.1029/2006GC001514, 2007.
- Linsley, B. K., Rosenthal, Y., and Oppo, D. W.: Holocene evolution of the Indonesian throughflow and the western Pacific warm Pool, *Nat. Geosci.*, 3, 578–583, 2010.
- Lo, L., Lai, Y.-H., Wei, K.-Y., Lin, Y.-S., Mii, H.-S., and Shen, C.-C.: Persistent sea surface temperature and declined sea surface salinity in the northwestern tropical Pacific over the past 7500 years, *J. Asian Earth Sci.*, 66, 234–239, 2013.

Millennial meridional dynamics of IPWP during the last termination

L. Lo et al.

Title Page

Abstract

Introduction

Conclusions

References

Tables

Figures



Back

Close

Full Screen / Esc

Printer-friendly Version

Interactive Discussion



Lo, L., Shen, C.-C., Lu, C.-J., Chen, Y.-C., Chang, C.-C., Wei, K.-Y., Qu, D., and Gagan, M. K.: Determination of element/Ca ratios in foraminifera and corals using cold- and hot-plasma techniques in inductively coupled plasma sector field mass spectrometry, *J. Asian Earth Sci.*, 81, 115–122, 2014.

5 McGee, D., Donohoe, A., Marshall, J., and Ferreira, D.: Changes in ITCZ location and cross-equatorial heat transport at the Last Glacial Maximum, Heinrich Stadial 1, and the mid-Holocene, *Earth Planet. Sc. Lett.*, 390, 69–79, 2014.

Meckler, A. N., Clarkson, M. O., Cobb, K. M., Sodemann, H., and Adkins, J. F.: Interglacial hydroclimate in the tropical West Pacific through the late Pleistocene, *Science*, 336, 1301–1304, 2012.

10 Melet, A., Verron, J., Gourdeau, L., and Koch-Larrouy, A.: Equatorial pathways of Solomon Sea water masses and their modification, *J. Phys. Oceanogr.*, 40, 810–826, 2011.

Mohtadi, M., Oppo, D. W., Steinke, S., Stuut, J.-B. W., De Pol-Holz, R., Hebbeln, D., and Lückge, A.: Glacial to Holocene swings of the Australian–Indonesian monsoon, *Nature Geosci.*, 4, 540–544, 2011.

15 Mothadi, M., Prange, M., Oppo, D. W., De Pol-Holz, R., Merkel, U., Zhang, X., Steinke, S., and Lückge, A.: North Atlantic forcing of tropical Indian Ocean climate, *Nature*, 509, 76–80, 2014.

20 Muller, J., Kylander, M., Wüst, R. A. J., Weiss, D., Martinez-Cortizas, A., LeGrande, A. N., Jennerjahn, T., Behling, H., Andreson, W. T., and Jacobson, G.: Possible evidence for wet Heinrich phases in tropical Australia: the Lynch's Crater deposit, *Quaternary Sci. Rev.*, 27, 468–475, 2008.

Northern Greenland Ice Core Project Members: High-resolution record of Northern Hemisphere climate extending into the last interglacial period, *Nature*, 431, 147–151, 2004.

25 Oppo, D. W., Rosenthal, Y., and Linsley, B. K.: 2,000-year-long temperature and hydrology reconstructions from the Indo-Pacific warm pool, *Nature*, 460, 1113–1116, 2009.

Pahnke, K., Zahn, R., Elderfield, H., and Schulz, M.: 340,000-year centennial-scale marine record of Southern Hemisphere climatic oscillation, *Science*, 301, 948–952, 2003.

30 Pena, L. D., Cacho, I., Ferretti, P., and Hall, M. A.: El Niño–Southern Oscillation-like variability during glacial terminations and interlatitudinal teleconnections, *Paleoceanography*, 23, PA3101, doi:10.1029/2008PA001620, 2008.

Qu, T., Gao, S., and Fine, R. A.: Subduction of South Pacific tropical water and its equatorward pathways as shown by a simulated passive tracer, *J. Phys. Oceanogr.*, 43, 1551–1565, 2013.

Millennial meridional dynamics of IPWP during the last termination

L. Lo et al.

[Title Page](#)[Abstract](#)[Introduction](#)[Conclusions](#)[References](#)[Tables](#)[Figures](#)[Back](#)[Close](#)[Full Screen / Esc](#)[Printer-friendly Version](#)[Interactive Discussion](#)

- Reimer, P. J., Baillie, M. G. L., Bard, E., Bayliss, A., Beck, J. W., Blackwell, P. G., Bronk Ramsey, C., Buck, C. E., Burr, G. S., Edwards, R. L., Friedrich, M., Grootes, P. M., Guilderson, T. P., Hajdas, I., Heaton, T. J., Hogg, A. G., Hughen, K. A., Kaiser, K. F., Kromer, B., McCormac, F. G., Manning, S. W., Reimer, R. W., Richards, D. A., Southon, J. R., Talamo, S., Turney, C. S. M., van der Plicht, J., and Weyhenmeyer, C. E.: INTCAL09 and MARINE09 radiocarbon age calibration curves, 0–50,000 cal BP *Radiocarbon*, 51, 1111–1150, 2009.
- Reynolds, R. W., Rayner, N. A., Smith, T. M., and Stokes, D. C.: An improved in situ and satellite SST analysis for climate, *J. Climate*, 15, 1609–1625, 2002.
- Rosenthal, Y., Oppo, D. W., and Linsley, B. K.: The amplitude and phasing of climate change during the last deglaciation in the Sulu Sea, western equatorial Pacific, *Geophys. Res. Lett.*, 30, 1428, doi:10.1029/2002GL016612, 2003.
- Shakun, J. D. and Carlson, A. E.: A global perspective on Last Glacial maximum to Holocene climate change, *Quaternary Sci. Rev.*, 29, 1801–1816, 2010.
- Shakun, J. D., Clark, P. U., He, F., Marcott, S. A., Mix, A. C., Liu, Z., Otto-Bliesner, B., Schmitzner, A., and Bard, E.: Global warming preceded by increasing carbon dioxide concentrations during the last deglaciation, *Nature*, 484, 49–55, 2012
- Shen, C.-C., Hasting, D. W., Lee, T., Chiu, C.-H., Lee, M.-Y., Wei, K.-Y., and Edwards, R. L.: High precision glacial–interglacial benthic foraminiferal Sr/Ca records from the eastern equatorial Atlantic Ocean and Caribbean Sea, *Earth Planet. Sc. Lett.*, 190, 197–209, 2001.
- Shen, C.-C., Chiu, H.-Y., Chiang, H.-W., Chu, M.-F., Wei, K.-Y., Steinke, S., Chen, M.-T., Lin, Y.-S., and Lo, L.: High precision measurements of Mg / Ca and Sr/Ca ratios in carbonates by cold plasma inductively coupled plasma quadrupole mass spectrometry, *Chem. Geol.*, 236, 339–249, 2007.
- Shiau, L.-J., Chen, M.-T., Clemens, S. C., Huh, C.-A., Yamamoto, M., and Yokoyama, Y.: Warm pool hydrological and terrestrial variability near southern Papua New Guinea over the past 50k, *Geophys. Res. Lett.*, 38, L00F01, doi:10.1029/2010GL045309, 2011.
- Shiau, L.-J., Chen, M.-T., Huh, C.-A., Yamamoto, M., and Yokoyama, Y.: Insolation and cross-hemispheric controls on Australian monsoon variability over the past 180 ka: new evidence from off shore southeastern Papua New Guinea, *J. Quaternary Sci.*, 27, 911–920, 2012.
- Steinke, S., Chiu, H.-I., Yu, P.-S., Shen, C.-C., Erlenkeuser, H., Löwemark, L., and Chen, M.-T.: On the influence of sea level and monsoon climate on the southern South China Sea freshwater budget over the past 22,000 years, *Quaternary Sci. Rev.*, 25, 1475–1488, 2006.

Millennial meridional dynamics of IPWP during the last termination

L. Lo et al.

[Title Page](#)

[Abstract](#)

[Introduction](#)

[Conclusions](#)

[References](#)

[Tables](#)

[Figures](#)

[◀](#)

[▶](#)

[◀](#)

[▶](#)

[Back](#)

[Close](#)

[Full Screen / Esc](#)

[Printer-friendly Version](#)

[Interactive Discussion](#)



- Stenni, B., Jouzel, J., Masson-Delmotte, V., Röthlisberger, R., Castellano, E., Cattani, O., Falourd, S., Johnsen, S. J., Longinelli, A., Sachs, J. P., Selmo, E., Souchez, R., Stefansen, J. P., and Udisti, R.: A late-glacial high-resolution site and source temperature record derived from EPICA Dome C isotope records (East Antarctica), *Earth Planet. Sc. Lett.*, 217, 183–195, 2003.
- Stott, L., Poulsen, C., Lund, S., and Thunell, R.: Super ENSO and global climate oscillations at millennial time scales, *Science*, 297, 222–226, 2002.
- Stott, L., Cannariato, K., Thunell, R., Haug, G. H., Koutavas, A., and Lund, S.: Decline of surface temperature and salinity in the western tropical Pacific Ocean in the Holocene epoch, *Nature*, 431, 56–59, 2004.
- Stuiver, M., Reimer, P. J., and Reimer, R. W.: CALIB 6.0. (WWW program and documentation), 2010.
- Visser, K., Thunell, R., and Stott, L.: Magnitude and timing of temperature change in the Indo-Pacific warm pool during deglaciation, *Nature*, 421, 152–155, 2003.
- Wang, X., Auler, A. S., Edwards, R. L., Cheng, H., Ito, E., Wang, Y., Kong, X., and Solheid, M.: Millennial-scale precipitation changes in southern Brazil over the past 90,000 years, *Geophys. Res. Lett.*, 34, L23701, doi:10.1029/2007GL031149, 2007.
- Wang, Y. J., Cheng, H., Edwards, R. L., An, Z. S., Wu, J. Y., Shen, C.-C., and Dorale, J. A.: A high-resolution absolute-dated late Pleistocene monsoon record from Hulu Cave, China, *Science*, 294, 2345–2348, 2001.
- Williams, A. P. and Funk, C.: A westward extension of the warm pool leads to a westward extension of the Walker circulation, drying eastern Africa, *Clim. Dynam.*, 37, 2417–2435, 2011.
- Xu, J., Holbourn, A., Kuhnt, W., Jian, Z., and Kawamura, H.: Changes in the thermocline structure of the Indonesian outflow during Terminations I and II, *Earth Planet. Sc. Lett.*, 273, 152–162, 2008.
- Yan, X.-H., Ho, C.-R., Zheng, Q., and Klemas, V.: Temperature and size variabilities of the western Pacific warm pool, *Science*, 258, 1643–1645, 1992.

Millennial meridional dynamics of IPWP during the last termination

L. Lo et al.

[Title Page](#)

[Abstract](#)

[Introduction](#)

[Conclusions](#)

[References](#)

[Tables](#)

[Figures](#)

[⏪](#)

[⏩](#)

[◀](#)

[▶](#)

[Back](#)

[Close](#)

[Full Screen / Esc](#)

[Printer-friendly Version](#)

[Interactive Discussion](#)



Table 1. AMS ^{14}C dates of site MD05-2925.

Depth (cm)	^{14}C ages (years)	Error (years)	Cal. ages (years)	Error (years)
117	8823	50	9414	111
127*	10 306	70	11 259	159
140	10 441	30	11 333	80
147*	11 477	70	12 854	110
157	12 066	60	13 391	84
172*	13 117	70	14 973	309
180	13 748	35	16 283	453
192*	14 080	74	16 746	223
207*	15 616	75	18 201	175
217	16 470	81	19 083	90
262*	18 985	94	22 167	181
272*	20 960	150	24 411	167
292*	21 650	78	25 304	339

* Samples were measured in the NSF-Arizona AMS Laboratory of the University of Arizona (U. Arizona), Tucson, USA, and the others were measured in the Rafter Radiocarbon Laboratory, Institute of Geological and Nuclear Science (GNS), New Zealand.

Millennial meridional dynamics of IPWP during the last termination

L. Lo et al.

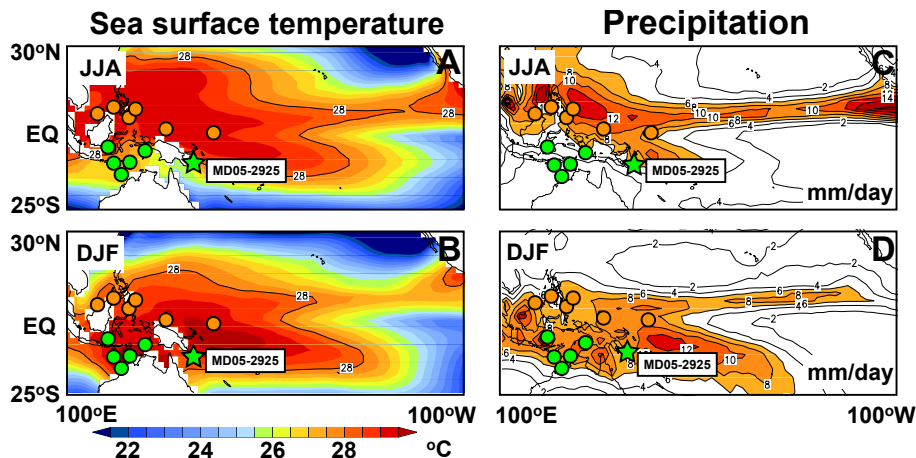


Figure 1. Climatological map of the Indo-Pacific Warm Pool (IPWP) sea surface temperature (SST, left) and precipitation (right) during 1950–2004 AD (Reynolds et al., 2002). Upper panels are June–July–August (JJA), and lower panels are December–January–February (DJF) averages of (A, C) SSTs and (B, D) precipitation distribution maps. SST and precipitation are at 0.5°C and 2 mm day^{-1} intervals. Our study site MD05-2925 is shown as the green star. Orange and green dots denote previous study sites in the IPWP region (Table 2) for reconstruction of meridional thermal and precipitation variations during the glacial/interglacial change.

[Title Page](#)
[Abstract](#)
[Introduction](#)
[Conclusions](#)
[References](#)
[Tables](#)
[Figures](#)
[Back](#)
[Close](#)
[Full Screen / Esc](#)
[Printer-friendly Version](#)
[Interactive Discussion](#)

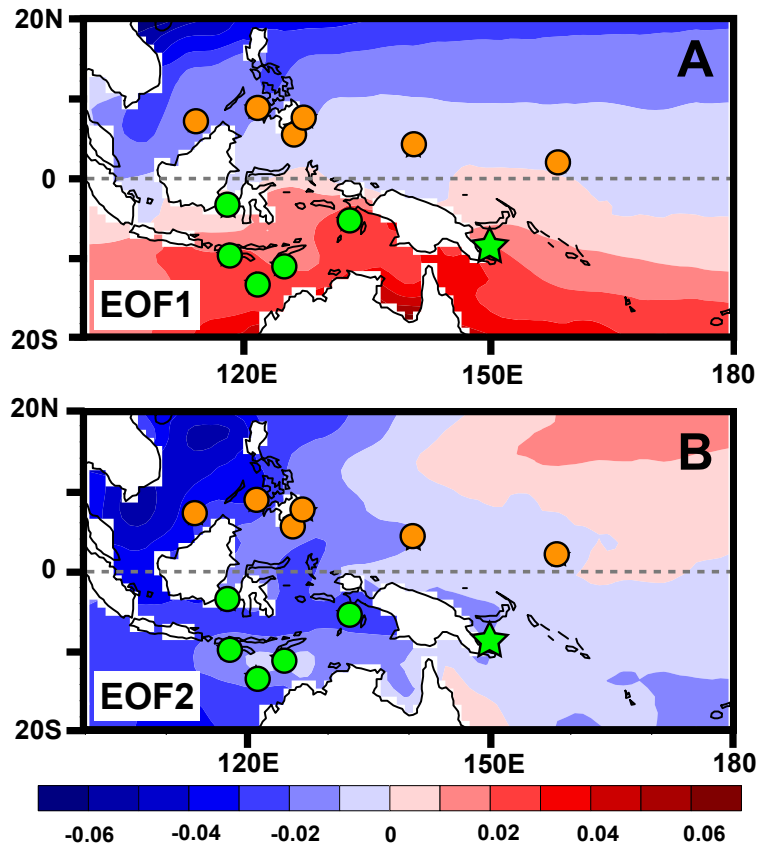


Figure 2. EOF analysis on SST (dataset from Reynolds et al., 2002) and selected sites (Table 2) used for stacked N- and S-IPWP records. **(A)** EOF1 explains 83.4 % of the total variance, which mainly represents intra-annual seasonality. **(B)** EOF2 shows a clear zonal pattern. Orange circles represent selected sites for the N-IPWP group and green ones for the S-IPWP group. The green star denotes the MD05-2925 site used in this study.

Millennial meridional dynamics of IPWP during the last termination

L. Lo et al.

Title Page

Abstract Introduction

Conclusions References

Tables Figures

◀ ▶

◀ ▶

Back Close

Full Screen / Esc

Printer-friendly Version

Interactive Discussion



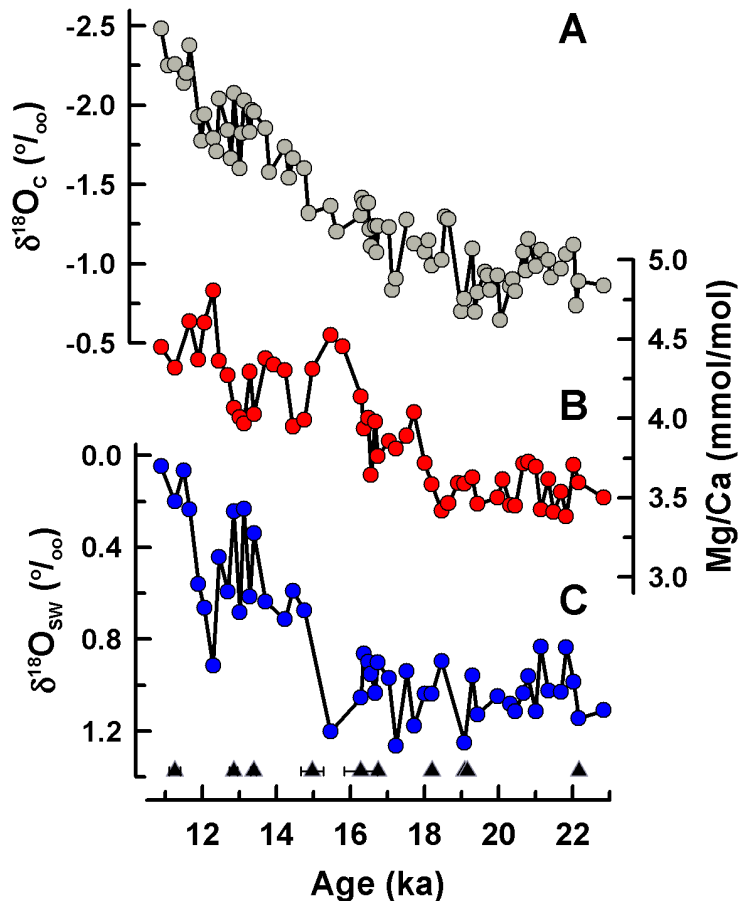


Figure 3. Planktonic foraminifera *G. ruber* geochemical proxy records of site MD05-2925, including (A) oxygen isotope ($\delta^{18}\text{O}_C$), (B) Mg / Ca ratio, and (C) temperature corrected-only sea-water oxygen isotope ($\delta^{18}\text{O}_{SW}$). Triangle symbols are corrected radiocarbon dates (Table 1).

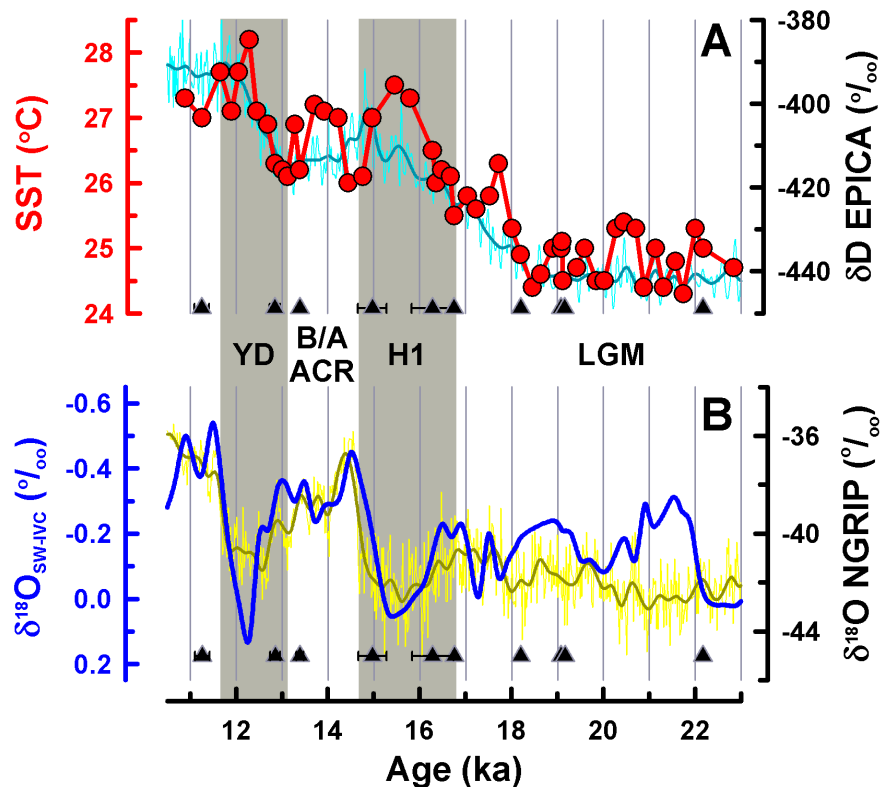


Figure 4. Geochemical proxy records of MD05-2925. **(A)** SST (red circles and line) and **(B)** $\delta^{18}\text{O}_{\text{SW-IVC}}$ (blue line) were reconstructed with *G. ruber* Mg/Ca ratios and $\delta^{18}\text{O}_{\text{C}}$. The cyan line denotes the Antarctica EPICA deuterium isotope record (Stenni et al., 2003), and the yellow line is the Greenland ice core NGRIP (Northern Greenland Ice Core Project Members, 2004) oxygen isotope record. The superimposed dark cyan and dark yellow lines are the 200 yr smoothed records, respectively. Black triangles are AMS ^{14}C dates (Table 1). Vertical bars denote the H1 and YD periods.

Millennial meridional dynamics of IPWP during the last termination

L. Lo et al.

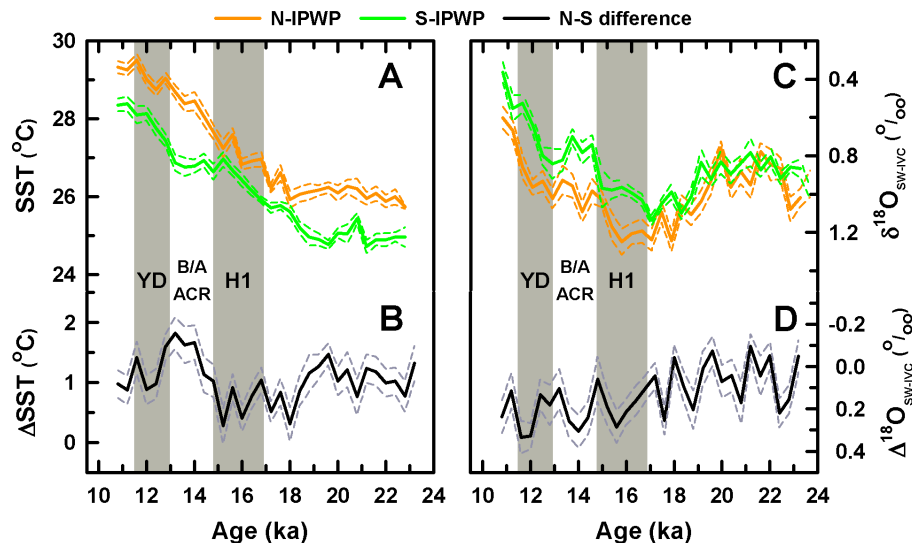


Figure 5. Four hundred-year non-overlapping binned (A) SST and (C) $\delta^{18}\text{O}_{\text{SW-IVC}}$ of N- (orange solid line) and S-IPWP (green solid line). Lower panels show the differences in (B) SST and (D) $\delta^{18}\text{O}_{\text{SW-IVC}}$ between N- and S-IPWP. The compilations of N- and S-IPWP surface water thermal and hydrological records (Table 2) were calculated with the non-overlapping binned methods (Oppo et al., 2009; Linsley et al., 2010). All dashed lines represent 1-sigma uncertainty ranges. Gray bars show the H1 and YD events.

Title Page

Abstract

Introduction

Conclusions

References

Tables

Figures

◀

▶

◀

▶

Back

Close

Full Screen / Esc

Printer-friendly Version

Interactive Discussion

Millennial meridional dynamics of IPWP during the last termination

L. Lo et al.

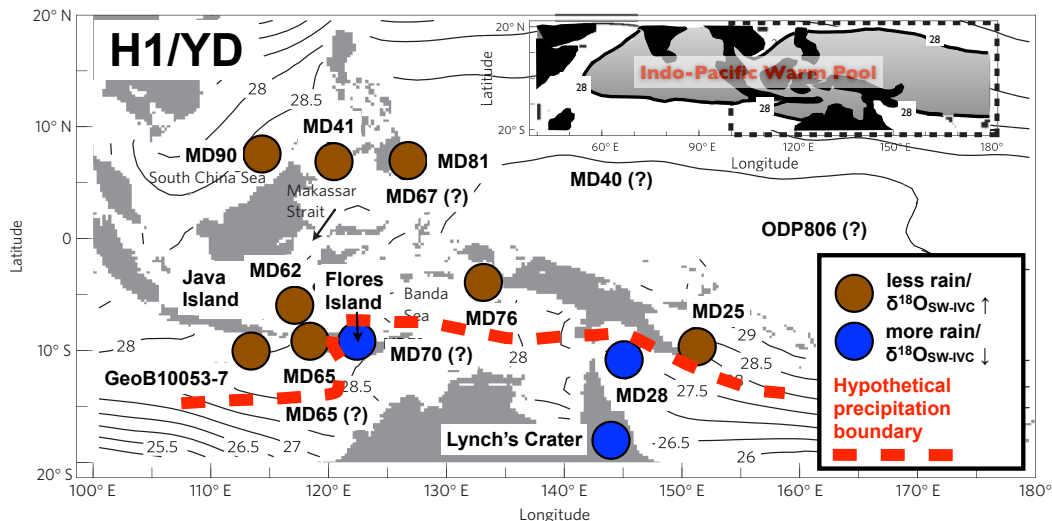


Figure 6. Hypothetical proxy-inferred precipitation boundary during the H1 and YD events (modified from the Linsley et al., 2010). Blue dots represent relatively increasing precipitation/ $\delta^{18}\text{O}_{\text{SW}}$ lighter condition, and brown ones a decreasing precipitation/ $\delta^{18}\text{O}_{\text{SW}}$ heavier condition. The segment between Java and Flores Islands of this sharp boundary (red dashed line) was proposed by Mohtadi et al. (2011), and the one between the Solomon and Coral Seas by this study. Black contours represent SST.

Title Page

Abstract

Introduction

Conclusions

References

Tables

Figures

◀

▶

◀

▶

Back

Close

Full Screen / Esc

Printer-friendly Version

Interactive Discussion

